THE ASTROPHYSICAL JOURNAL, 193:481–493, 1974 October 15

THE THERMAL STRUCTURE OF THE ATMOSPHERE OF JUPITER

L. WALLACE, MICHAEL PRATHER,* AND MICHAEL J. S. BELTON
Kitt Peak National Observatory†
Received 1974 March 14; revised 1974 May 23

ABSTRACT

Radiative equilibrium models of the Jovian atmosphere calculated by Hogan, Rasool, and Encrenaz and by Cess and Khetan are shown to be in conflict. A new calculation is presented which agrees closely with that of Cess and Khetan. This model, however, fails to predict the observed intensity in the 7.8-μ CH_4 band by about a factor of 8. Approximate heating rates are calculated for CH_4 band complexes between 0.6 and 7.8 μ and for various distributions of high-altitude aerosol heating. Temperature profiles are computed for these heating rates. It is shown that the observed emission intensity in the 7.8-μ band is a critical test of these models. The temperature profile based on CH_4 heating alone predicts an emission intensity in the band which is within 25 percent of the observed value. Aerosol heating is not excluded, provided it is very deep or broadly distributed in the atmosphere. In addition, the model based on CH_4 heating alone is shown to give good agreement with the observed center-to-limb observations at 7.94 μ. To obtain agreement between model prediction and the observed emission intensity at 8.5 μ, it is necessary to include an extra broad-band opacity, presumably a cloud. A comparison with the results of the β Sco occultation could indicate the presence of a high-altitude cooling agent. Ethane, ethylene, and acetylene are all shown to reduce the stratospheric temperature slightly relative to that characteristic of CH_4. It is shown that, in order to simultaneously maintain the agreement between the models and the β Sco occultation and the emission intensity at 7.8 μ, the He/H_2 ratio must be kept small ($\ll 0.5$) if the observed CH_4 abundance is correct. The *Pioneer 10* radio occultation profile is at variance with the models. The emission intensity at 7.8 μ implied by the *Pioneer 10* result is shown to be 100 times greater than observed. We conclude that the *Pioneer 10* temperature profile is not representative of the global average.

Subject headings: atmospheres, planetary — Jupiter

I. INTRODUCTION

The thermal structure in the upper troposphere and lower stratosphere of a planet is determined by a local balance between radiative heating and cooling and the redistribution of energy by motions or waves. In the Earth's troposphere, Stone (1972) has shown that large-scale horizontal advection of heat is very important in determining the temperature structure. In the case of the Jovian troposphere, which should be much less stable, large-scale motions are not expected to be so important, and a simple radiative-convective calculation should be adequate (Trafton and Stone 1974). In the stratosphere the inclusion of large-scale motions may be decisive if the planetary rotation is slow and the thermal response time is short; the rapid superrotation of the Venus stratosphere may be the best example of this (Schubert and Young 1970; Gierasch 1970). For a rapidly rotating planet like Jupiter, in which the thermal response time in the atmosphere is also relatively long, the drives for large-scale motions are minimized (Schubert and Young 1970) and a simple radiative equilibrium calculation may be adequate to characterize the atmosphere structure. Deposition of energy in the high stratosphere by dissipating waves generated by motions at lower altitudes could be important. (French and Gierasch 1974); but because this process is poorly understood and difficult to parametrize, it is best put to one side until required for an explanation of some otherwise inexplicable observation.

In this paper we present new radiative equilibrium models, which neglect large-scale dynamical processes, and we test those models against various observational constraints. The models are appropriate at pressures greater than 10 dyn cm^{-2} where non–LTE effects are unimportant. Previous model calculations were inspired by the spectrum of Jupiter (Gillett, Low, and Stein 1969) in the 2.8–14 μ region which shows a minimum brightness temperature of $\sim 115°$ K increasing to $\sim 145°$ K in the 7.8-μ CH_4 band. Gillett *et al.* concluded that the atmospheric temperature must first decrease with increasing height to 115° K or less and then rise again in an inversion to no less than 145° K. They proposed that high-altitude solar heating in the 3.3-μ CH_4 band with subsequent reradiation in the 7.8-μ CH_4 band maintains this inversion. Hogan, Rasool, and Encrenaz (1969) have calculated radiative equilibrium models for Jupiter which include these two methane bands, and they find a temperature inversion with a maximum of about 140° K. But more recently Cess and Khetan (1973) have considered the same problem and find the temperature inversion to occur at pressures which are about a factor of 10 lower than Hogan *et al.* In § II we reevaluate this problem and find good agreement with the results of Cess and Khetan. In §§ III and IV, heating due to weaker methane bands and to aerosols is added. The final section compares calculated and observed emission

* Summer Research Assistant from Yale University Observatory.

† Kitt Peak National Observatory is operated by the Association of Universities for Research in Astronomy, Inc., under contract with the National Science Foundation.

intensities in the 7–14 μ region and then compares calculated and observed temperature profiles derived from the β Sco and *Pioneer 10* occultations. This section also demonstrates that the calculated intensity of the 7.8-μ methane band provides a critical test for both calculated and observed temperature profiles.

II. CALCULATION OF THE TEMPERATURE STRUCTURE WITH THE 3.3- AND 7.8-MICRON BANDS

a) Method

With the assumption of radiative equilibrium, LTE, and negligible scattering, the radiant intensity at pressure p and wavenumber ω is given by

$$I(\omega, \mu, p) = -\int_{p'=p}^{\text{limit}} B(\omega, p')d\{\exp[-\theta(\omega, \mu, p, p')]\} . \tag{1}$$

The direction cosine relative to the normal is μ, the appropriate limit is 0 or ∞ depending on whether μ is positive or negative, B is the Planck function, θ is the slant opacity between p and p', and the flux πF can be derived from the relation

$$F(p) = \int F(\omega, p)d\omega = 2\int\int_0^1 [I(\omega, +\mu, p) - I(\omega, -\mu, p)]\mu d\mu d\omega . \tag{2}$$

The integrals in equation (2) were reduced to quadratures, and the required quantities (B and θ) were calculated at a grid of pressure points p_i. The integrals in equation (1) were evaluated analytically between pressure points on the assumption that $B(\omega)$ varies linearly with $\theta(\omega)$. The density of grid points p_i can readily be increased to the point where this assumption introduces insignificant error. The flux carried by the atmosphere was taken as

$$\mathscr{F}(p) = \frac{\mu_0}{2R^2}\sum_{\omega} F_\omega \Delta\omega \exp[-\theta(\omega, \mu_0, p, 0)] + \text{constant} . \tag{3}$$

The quantity πF_ω is the solar flux at 1 a.u., μ_0 is the cosine of the latitude, the factor of 2 converts to average diurnal insolation, and R is the Sun-planet distance in a.u. The summation was taken to include the 3.3- and 7.8-μ bands of CH_4. The constant was selected to make $\mathscr{F}(0) = \sigma T_e^4/\pi$, where T_e is the assumed effective temperature. This constant represents the internally generated energy flux and the incident solar flux which is deposited below the region of the atmosphere being treated here.

Flux errors generated from equation (1) and a trial temperature run were used to obtain temperature corrections, $\Delta T(p_j)$, by assuming that

$$\mathscr{F}(p_i) = F(p_i) + \sum_j \frac{\partial F(p_i)}{\partial T(p_j)} \Delta T(p_j) . \tag{4}$$

Several iterations were required to obtain convergence. After five or six iterations, $|\Delta T| \sim 0.01°$ K and the fractional flux errors were $\sim 10^{-5}$. An additional three or four iterations reduces the flux errors to $\sim 10^{-13}$ to 10^{-14}, the accuracy of the computer. In the calculations we found it necessary to include the temperature dependence in the pressure-induced absorption coefficient but not that of the methane bands. Also, to avoid a sawtooth pattern in the temperatures at low pressures, it was necessary to offset, in pressure, the temperature grid points from the flux points.

The translational parts of the pressure-induced opacity due to H_2:He mixtures were calculated from the parameters given by Trafton (1965, 1966). The translation-rotation and translation-rotation-vibration parts were calculated following Linsky (1969). The "exponential" extrapolation of the absorption coefficients was used since the "power law" extrapolation appears to be ruled out (Belton and Spinrad 1973).

Computational runs were made with increasing numbers of grid points, the last having six points in angle and four temperatures per decade in pressure. The greatest difference between the results with the coarsest and finest grids was 3° K, indicating that further refinement of the grid would not alter the results by more than $\sim 1°$ K.

The results for a pure H_2 atmosphere and one with an [He]/[H_2] number mixing ratio of unity agree with those of Trafton (1965) to within 3° K for a frequency grid with 10 points distributed uniformly in ω from 0 to 500 cm^{-1} and an additional nine from 500 to 1400 cm^{-1}. Since doubling the number of points in ω does not improve the agreement, we conclude that the 3° K difference is due to our different handling of the translation-rotation and translation-rotation-vibration opacities.

Random band models (Goody 1964, chap. 4) were used to represent methane broad-band opacities. Line parameters were taken from Kyle (1968) and pressure-broadening widths from Varanasi (1971) and Varanasi and Tejwani (1972). The solar fluxes of Labs and Neckel (1968) were used for the heating rates.

Plots of cumulative line strengths showed that a model in which the probability of line strength S is proportional to S^{-1} was much more appropriate than the exp $(-S/\sigma)$ model used by Taylor (1972*a*). We found that for lines with Doppler profiles the exp $(-S/\sigma)$ model can lead to as much as a factor of 2 error in the opacities.

A simple analytic expression, accurate to 0.5 percent, for the mean opacity θ_L over an inhomogeneous path, due to Lorentz lines in the S^{-1} model was obtained by approximating the exact expression for a homogeneous slab (Goody 1964) and then applying the Curtis-Godson approximation. The result is

$$\theta_L = 2\pi y F(u)\,, \tag{5a}$$

where

$$F(u) = u(1 + 0.515u)^{-1/2}\,, \qquad u \leq 4\,, \tag{5b}$$

$$F(u) = (0.5 + 4u - 0.03125/u)(2\pi u)^{-1/2} - 1\,, \qquad u > 4\,, \tag{5c}$$

$$u = \frac{2}{\pi}\left[\frac{\sum \int S da}{\sum (\int S\alpha_L da)^{1/2}}\right]^2 \quad \text{and} \quad y = \frac{1}{4\Delta\omega}\frac{[\sum (\int S\alpha_L da)^{1/2}]^2}{\sum \int S da}\,. \tag{6}$$

The summations are over all the lines in the wavenumber interval $\Delta\omega$, α_L is the Lorentz width, and a is the slant amount of absorber.

To calculate the mean opacity θ_D for Doppler lines, we first found approximations for the equivalent width of a single line for a homogeneous slab, accurate to 1 percent, and then performed the integration appropriate to the S^{-1} model to obtain

$$\theta_D = 2vG(w)\,, \tag{7a}$$

where

$$G(w) = 3.8035\left[\ln\left(\frac{w + 3.4097}{w + 16.5903}\right) + 1.5822\right]\,, \quad w \leq 4\,; \tag{7b}$$

$$G(w) = 0.1462 + \tfrac{2}{3}\ln^{3/2}(\pi^{1/2}w) + 0.3073/\ln(\pi^{1/2}w)\,, \quad w > 4\,; \tag{7c}$$

$v = K\alpha_D/\delta$, $w = S_{max}a/(\pi^{1/2}\alpha_D)$, α_D is the Doppler width, K is a constant, and S_{max} is the line strength of the strongest line. Since the temperature does not vary strongly, we used the temperature at the bottom of the column concerned to calculate α_D. K and S_{max} were determined for the Doppler shape requiring that the sum of the strengths and sum of the square root of the strengths be the same for the actual strengths and the model. This is arbitrary but gives good results. For the inhomogeneous path

$$w = \frac{4}{\alpha_D\pi^{1/2}}\left[\frac{\sum \int S da}{\sum (\int S da)^{1/2}}\right]^2 \quad \text{and} \quad v = \frac{\alpha_D}{4\Delta\omega}\frac{[\sum (\int S da)^{1/2}]^2}{\sum \int S da}\,. \tag{8}$$

The combined opacity, θ_{LD}, was taken as $\theta_{LD} = (\theta_L^2 + \theta_D^2)^{1/2}$. Otherwise θ_{LD} was taken equal to the larger of θ_L and θ_D. This combined Lorentz/Doppler model was compared with the more accurate result of combining, in the manner prescribed by the random band model, the equivalent widths of the actual lines. The error maximized at 10 percent when $\theta_L \sim \theta_D$ and decreased rapidly as one or the other of θ_L or θ_D dominated.

The question of the validity of using a Lorentz shape to approximate pressure-broadened profiles for methane has been raised by Taylor (1972*a*). For ammonia, departures from the Lorentz shape are complicated (Trafton

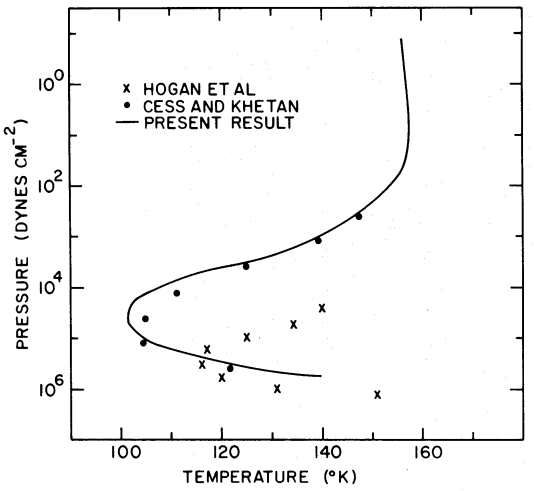

FIG. 1.—A comparison of Jovian temperature profiles computed by Hogan *et al.* (1969), Cess and Khetan (1973), and the present authors. All three include heating and cooling in the 3.3- and 7.8-μ bands of methane, and have the same chemical composition and similar effective temperatures.

1973; Varanasi 1972). For methane, Varanasi (1971) and Varanasi and Tejwani (1972) show that the Lorentz shape provides an accurate description of the variation of the absorption coefficient between the line centers. The question of the extrapolation to wavenumbers large compared with the line separation ($\sim$hundreds of cm^{-1}) is a different matter on which there appears to be no direct observational evidence. In our band model, however, the Lorentz wings of the lines in a specific interval $\Delta\omega$ are assumed to be confined to that interval, which is analogous to the assumption that the far wings are sub-Lorentzian (see Gille and Lee 1969).

b) Results

In figure 1 we compare the temperature structure obtained by Hogan *et al.* (1969) for their model 3 with the present result for the same model. The model has $T_e = 127°$ K, $[He]/[H_2] = 0.2$, $[CH_4]/[H_2] = 10^{-3}$, and diurnal average solar illumination at 45° latitude.

The agreement is very poor. Hogan *et al.* have other models which show temperature inversions and one which shows no inversion at all. All of these are in disagreement with the present results. Figure 1 also shows a model by Cess and Khetan (1973) which differs from the others only in having $T_e = 120°$ K and being for a diurnal average solar illumination at 0° latitude. The agreement with the present results is very good and, since the approach of Cess and Khetan is very different from ours, is hardly due to common errors. The agreement between the present results and those of Cess and Khetan in the region of the inversion and those of Trafton (1965, 1967) in the greenhouse region convinces us that our results cannot be substantially in error. Dr. Hogan has informed us that he is obtaining new results that are more in agreement with those of Cess and Khetan.

In order to compare model predictions with the observed spectrum (§ V), we calculated a model (fig. 2) for $T_e = 134°$ K, the result obtained from broad-band flux measurements (Aumann, Gillespie, and Low 1969). Diffusive separation of methane was included in the manner of Wallace and Hunten (1973) assuming an eddy diffusion coefficient of 5×10^5 cm^2 s^{-1} and $[CH_4]/[H_2] = 7 \times 10^{-4}$ at great depths, consistent with solar abundance. The inclusion of diffusion is of no consequence to the present results since diffusive separation occurs only above $p \sim 1$ dyn cm^{-2}, but it has the practical advantage of increasing the pressure at which the cores of the lines become thin and thereby reducing the number of grid points in pressure. The ratio $[He]/[H_2]$ was assumed constant at 0.11 (Hunten and Münch 1973).

III. HEATING BY WEAKER CH_4 BANDS

Weak bands shortward of 3.3 μ contribute little to the heating at very low pressures, but at higher pressures where the strong bands have saturated and no longer contribute to the local heating they become important.

a) Method

Since the majority of these bands have not been analyzed, we abandon the approach used for the 3.3- and 7.8-μ bands, neglect temperature dependence, and adopt the simpler $\exp(-S/\sigma)$ model (Goody 1964, chap. 4). Three parameters are needed: a total intensity for the group of lines, the number of lines, and the characteristic width of the band, $\Delta\omega$.

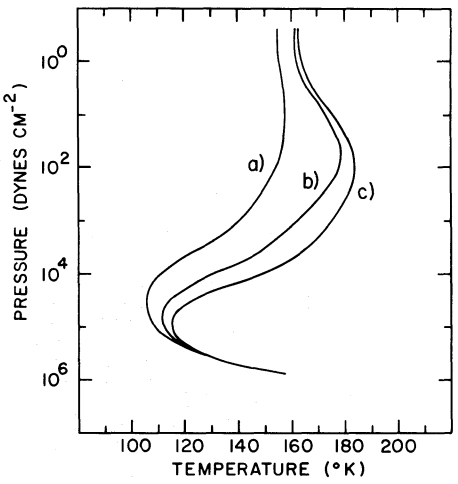

FIG. 2.—Models computed for an effective temperature of 134° K. The three models, which show progressively higher stratospheric temperatures, include (*a*) only the 3.3- and 7.8-μ bands, (*b*) the additional heating due to weaker bands (model I), and (*c*) heating due to "dust" distributed according to eq. (12) with $N_0 = 2.1 \times 10^{22}$ cm^{-2}. This was chosen to produce an intensity in the 7.8-μ band similar to that reported by Gillett *et al.* (1969).

The laboratory spectra of Kuiper and Cruikshank (1964) for the 1–2.5 μ region show two band complexes centered at 1.7 and 2.3 μ. We treat each of the complexes as an entity and estimate $\Delta\omega$ as 700 and 730 cm^{-1}, respectively. The total intensity S of the single band at 1.67 μ is 1.0 cm^{-1}/(cm amagat) (Goody 1964). Since there appear to be two other bands of similar intensity in the 1.7-μ group, we estimate a strength of 3 cm^{-1}/(cm amagat) for this complex. In order to obtain agreement with the data of Kuiper and Cruikshank, the total number of lines in the group was taken as 300. The 2.3-μ complex seems to consist of four bands. We therefore assume the number of lines to be 400 and obtain an intensity for the complex of 25 cm^{-1}/(cm amagat).

The semiempirical approximation used for mean slant opacity with the exp $(-S/\sigma)$ model which includes both the Lorentz and Doppler shapes is

$$\theta_{LD} = \frac{2\alpha_D}{\delta}\frac{\eta}{\eta + 1 + \beta}\{\ln[\eta + \exp(\pi/4)] + (\eta + 2 + \beta)\beta\pi/4\}^{1/2}, \tag{9}$$

where

$$\eta = \frac{\sigma a}{\pi^{1/2}\alpha_D} \quad \text{and} \quad \beta = \frac{\pi^{1/2}\alpha_L}{\alpha_D} \tag{10}$$

and the other parameters are defined above. Comparison with calculations using Voigt profiles and the assumption of random spacing indicates that this approximation is in error by no more than 4 percent.

For the still weaker bands shortward of 1.5 μ, a different approach was used because of the lack of laboratory data. Doppler broadening was neglected entirely since it is only marginally significant at low pressures where the heating rates are dominated by much stronger bands. Consequently, we used Goody's exact exp $(-S/\sigma)$ model for Lorentz profiles, which for a constant mixing ratio reduces to

$$\theta_L = Ca, \tag{11}$$

where C is a constant at each wavelength. Since C and the total column amount above the apparent cloud deck, a_1, along with the albedo of the cloud deck λ_0 define the geometric albedo of the planet, it is a straightforward process to convert observed geometric albedos into C's. For that purpose we assume a reflecting layer model with $a_1 = 6 \times 10^3$ cm amagat of CH_4 in the slant path at $\mu = 0.5$ (Belton 1969), $\lambda_0 = 0.83$ corresponding to the maximum observed albedo at about 6000 Å and the spectral observations of Jupiter between 0.6 and 1.5 μ by Danielson (1966) and Pilcher, Prinn, and McCord (1973). This procedure has the defect that absorptions due to gases which are not uniformly mixed, such as ammonia, as well as pressure-induced absorptions, are incorrectly included. In the spirit of these calculations, however, such errors are inconsequential. The values of C derived in this manner and used in the calculations are given in table 1.

b) Results

The heating rates for the 1.7- and 2.3-μ complexes are compared with those for the 3.3- and 7.8-μ bands in figure 3. Both have the same character. For small enough amounts (fig. 3, *top*), the lines are optically thin and the heating rate is constant. As the Doppler cores become saturated, the heating rates fall off. This decrease continues until the opacity in the Lorentz wings is more important than that in the cores. Then the heating rate is again constant until the overlapped Lorentz wings saturate and the heating rate falls off indefinitely. The contribution from the bands shortward of 1.5 μ is also indicated in figure 3. This contribution does not fall off much at high pressure since the slant opacity in most of the bands remains small. As might be anticipated, the strong bands contribute most at low pressure while the weak bands dominate at high pressure.

The temperature profile for $T_e = 134°$ K and which includes the heating due to these weaker bands is shown in figure 2. We subsequently refer to this profile as model I.

TABLE 1

THE PARAMETERS C USED TO DETERMINE THE HEATING RATES ASSOCIATED WITH BAND ABSORPTION AT WAVELENGTHS LESS THAN 1.5 MICRONS

$\lambda(\mu)$	C	$\lambda(\mu)$	C	$\lambda(\mu)$	C
0.74	3.1 (−5)	0.98	1.2 (−4)	1.25	7.0 (−5)
0.78	3.1 (−5)	1.02	9.8 (−5)	1.30	1.7 (−4)
0.82	1.3 (−5)	1.06	2.9 (−5)	1.35	4.7 (−4)
0.86	3.9 (−5)	1.10	5.3 (−5)	1.40	2.7 (−4)
0.90	8.3 (−5)	1.15	1.8 (−4)	1.45	1.1 (−4)
0.94	1.3 (−5)	1.20	6.7 (−5)	1.50	5.2 (−5)

NOTE.—The units of C are (cm amagat)$^{-1}$.

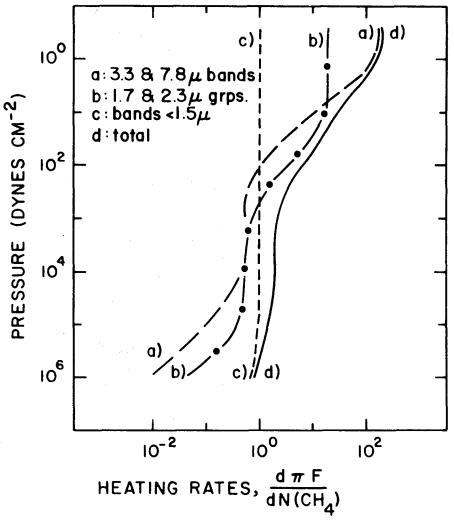

FIG. 3.—Heating rates for different groups of methane bands. The units on the abscissa are ergs cm^{-2} s^{-1} per cm-amagat of methane.

IV. HEATING BY "DUST"

The albedo of Jupiter decreases from 6000 to 4000 Å and then remains more or less constant to at least 2000 Å (Anderson *et al.* 1969; Wallace, Caldwell, and Savage 1972). Axel (1972) has suggested that this short-wavelength absorption could be an important heating source. The nature of the absorber is unknown, but Axel thought of it as dust while Strobel (1973*b*) has suggested condensed hydrazine (N_2H_4), a by-product of the ammonia photochemistry.

The observed albedo implies that 0.15 of the incident solar flux is deposited in the atmosphere by this mechanism, but the distribution of heating with height is quite unknown. We arbitrarily assume, for this preliminary assessment, that the solar flux varies as

$$F = \frac{F_0}{4R^2} \frac{1}{1 + N(CH_4)/N_0} \tag{12}$$

through the atmosphere. The incident flux πF_0 is 2×10^5 ergs cm^{-2} s^{-1}, and $N(CH_4)$ is the methane column density. The flux deposition is essentially constant down to $N(CH_4) = N_0$ and then cuts off in a manner chosen

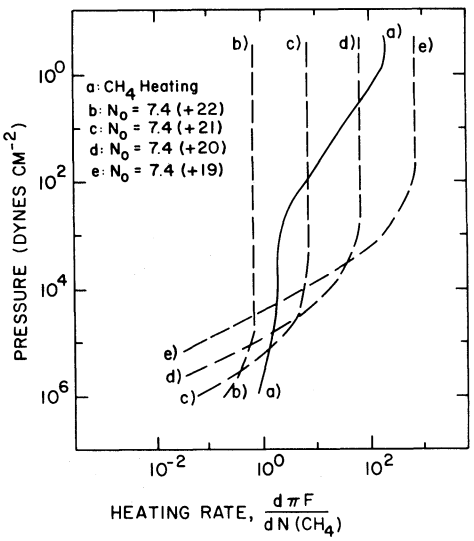

FIG. 4.—A comparison of heating rates due to all the methane bands (curve *a*) with that due to the blue-violet, or "dust" heating parametrized according to eq. (12). The units of the abscissa are the same as in fig. 3.

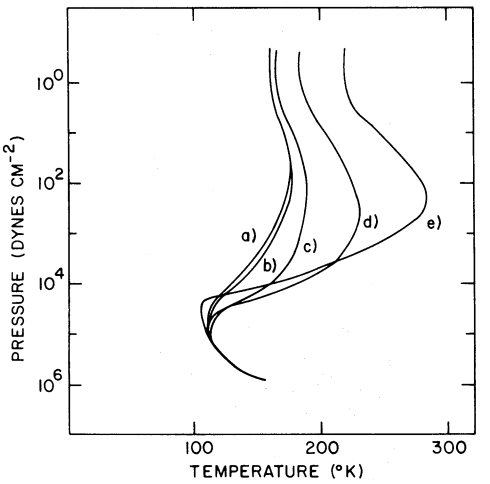

FIG. 5.—Temperature profiles computed using the heating rates shown in fig. 4. Curve (*a*) is for heating due to methane only (model I). The other curves are designated by the same letters as in fig. 4.

to avoid numerical problems. We neglect thermal reemission by the dust, primarily because it represents yet another unknown, but also because we are interested in the maximum possible effect of this type of heating. Heating rates for this distribution are compared with the total methane heating rate in figure 4. It is apparent that if the heat were distributed uniformly down to a pressure of 0.1 atm (curve *b* or *c*) or deeper, it would have little effect since it would be less than or comparable to the methane heating. Thermal models for these distributions, with the total methane heating included, are given in figure 5. They are two-stream models with two temperature determinations per decade of pressure and are more uncertain than the other models. They do, however, indicate that temperatures $\sim 250°$ K can be obtained above a pressure level of 3×10^4 dyn cm^{-2} if the heat is not deposited too low.

We have also examined a second possibility in which the heating is localized in relatively narrow pressure ranges. The heating rates and resulting thermal structures are given in figures 6 and 7. Heating rates labeled (*a*)–(*e*) yield temperature profiles (*a*)–(*e*), respectively. Curve (*a*) is model I; the rest of the curves include dust heating. Heating distribution (*b*) produces less of a temperature increase than (*c*) because the energy is deposited deeper. This is because the heating per gram is less and the ability to radiate per gram is greater since the pressure-induced absorption coefficient is proportional to the square of the number density.

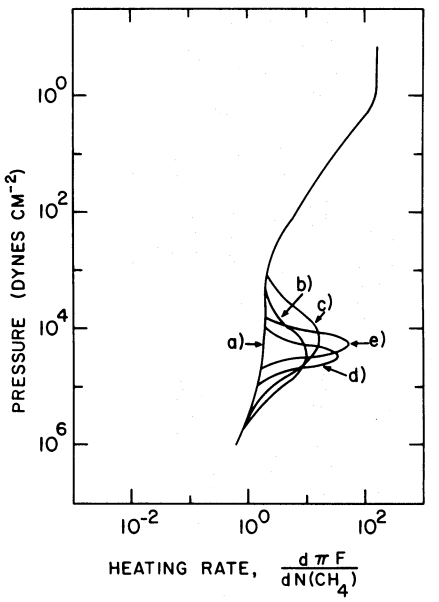

FIG. 6.—Heating rates which assume a peaked distribution for the deposition of energy associated with the low blue-violet albedo. Curve (*a*) is for total methane heating alone. The units of the abscissa are the same as in fig. 3.

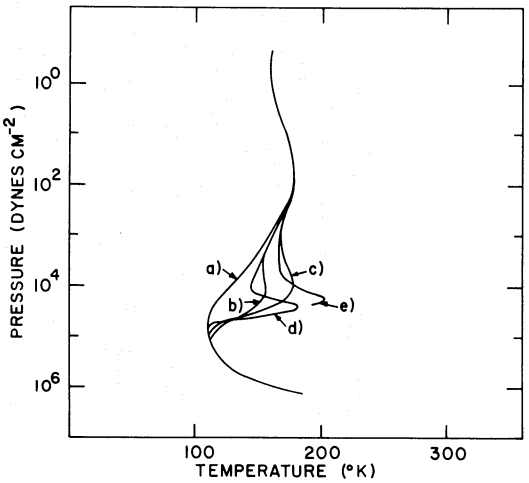

FIG. 7.—Temperature profiles computed using the heating rates shown in fig. 6. The curves are designated by the same letters as in fig. 6.

These models were evaluated with eight grid points per decade in pressure instead of the usual four. Even so, the thermal calculation for heating curve (*e*) did not converge in the pressure interval 3×10^4 to 10^5 dyn cm^{-2}. The calculations indicate, however, that temperatures as high as 200° K can be achieved at pressures as high as 3×10^4 dyn cm^{-2} if the heating is sufficiently localized. Since we have neglected the ability of the "dust" to radiate, the derived temperatures are upper limits. We also note that an indefinitely high temperature could be attained if the heating were confined to an indefinitely narrow pressure interval. But presumably convective transport would take over at some point to wipe out such a temperature spike.

V. DISCUSSION

a) Comparison with the 7- to 14-μ Spectrum of Gillett, Low, and Stein

The emission intensity in the 7- to 14-μ region is illustrated in figure 8. Consider first wavelengths $\lambda \geq 8.5\ \mu$. The upper curve was calculated from model I but with a semi-infinite convective atmosphere grafted on at the

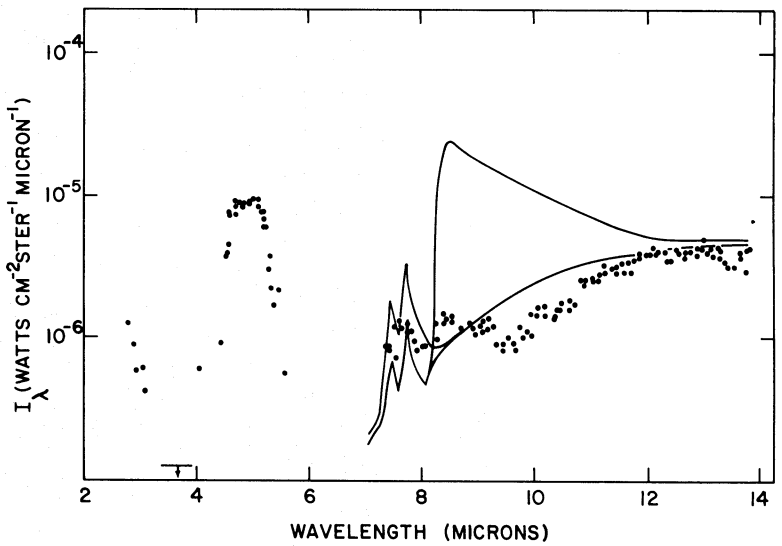

FIG. 8.—Comparison of the spectrum observed by Gillett *et al.* (1969) with model spectra. All models have an effective temperature of 134° K. At 8.5 μ, the more intense spectrum is for a clear He:H_2 atmosphere. The less intense spectrum is based on a model with a dense cloud at a temperature of 135° K. At 8.5 μ, the effect of upper atmospheric heating is negligible. The inclusion of ammonia absorption would depress both models in the 9- to 12-μ region. From 7 to 8 μ, the computed spectra are dominated by the 7.8-μ methane band. The less intense of the two is based on model I (curve *b*, fig. 2) which only includes heating due to methane. The more intense spectrum is based on curve (*c*), fig. 2, which includes heating associated with the low blue-violet albedo.

point where the radiative temperature gradient surpassed the adiabatic gradient (Trafton 1967). The agreement with observation is satisfactory between 12 and 13 μ, but rapidly deteriorates to short wavelengths. At 8.5 μ the model predicts intensities which are a factor of 20 too high. The steep rise from 14 to 8.5 μ results from the decreasing opacity of the He/H_2 mixture. This effect is not very sensitive to $[He]/[H_2]$. The more recent Jupiter spectrum observed by Aitken and Jones (1972) has a higher resolution than that of Gillett *et al.* and shows the 10-μ NH_3 band with identifiable lines from 9 to 12 μ. We have not included absorption by NH_3 in our models, but it is unlikely that it could depress the continuum by a factor of 20 at 8.5 μ and have only a minor effect at 10 μ where the absorption is strongest. Methane absorption is negligible at 8.5 μ. It is also unlikely that the pressure-induced opacity could be so wrong at 8.5 μ as to produce a factor of 20 error. We conclude that either an unknown absorber is present or a cloud is involved. We note, however, that in the model spectra calculated by Encrenaz (1972) based on the suspect thermal models of Hogan *et al.* the intensity of the continuum in this region decreases, corresponding to an approximately constant brightness temperature, as required. This is probably because in the models of Hogan *et al.*, $\theta \sim 1$ occurs in the temperature minima, instead of deeper in a region where the temperature is increasing inward.

The possible influence of a cloud is illustrated by the lower curve in figure 8 at wavelengths $\lambda \geq 8.5$ μ. We assume model I but with dense cloud with unit emissivity at the 135° K level. In this picture the inclusion of ammonia absorption could reasonably decrease the continuum level in the 9- to 12-μ region to enhance the agreement.

At wavelengths short of 8 μ the methane opacity in the 7.8-μ band dominates. The calculated spectra are for 20 cm^{-1} resolution, approximately that of the observations. In the spectrum, derived from model I, the intensity is only ~25 percent lower than observed. We consider this agreement entirely satisfactory. With the model in which only the 3.3- and 7.8-μ bands are included (curve *a* of fig. 2), the 7.8-μ intensity is about a factor of 8 lower than the observations. The model that includes "dust" heating according to equation (12) with $N_0 = 2.1 \times 10^{22}$ (curve *c* of fig. 2) yields the upper curve in figure 8 at wavelengths shortward of 8 μ. This model is a little too hot but not unacceptable. Spectra derived from the hotter "dust" models (curves *c*, *d*, and *e* of figs. 4 and 5) yield intensities in the 7.8-μ band which are too large by factors of 5, 30, and 60. Models with peaked distributions of "dust" (curves *b–e* of figs. 6 and 7) give intensities in this band which are too large by factors of 1.7, 5, 4, and 10, respectively.

Apparently, "dust" heating is not required in the models to achieve agreement with the observed 7.8-μ band. If present, the net heating from this source must be distributed in such a way that the effect on the temperature structure is not much greater than that illustrated in curve (*b*) of figure 5 or curve (*b*) of figure 7.

The region from 7.7 to 8.5 μ was discussed by Gillett *et al.* (1969) from the idealized view that the observed brightness temperature was roughly equal to the actual temperature at the $\theta \sim 1$ level. Proceeding from 8.5 to 7.7 μ, the observed intensity dip through a spectral region of increasing methane opacity was interpreted as a temperature minimum in the atmospheric structure. While our models agree with their deduction, the assumption that the observed emission arises from a relatively narrow region of the atmosphere near $\theta = 1$ is not necessarily correct if there is a substantial temperature inversion. The effect is illustrated in figure 9, which shows the contributions to the emergent intensity from different levels in a 20 cm^{-1} wide band centered at 8.05 μ. The figure is based on model I with a cloud at 135° K. To achieve the decomposition, we split equation (1) into a sum of

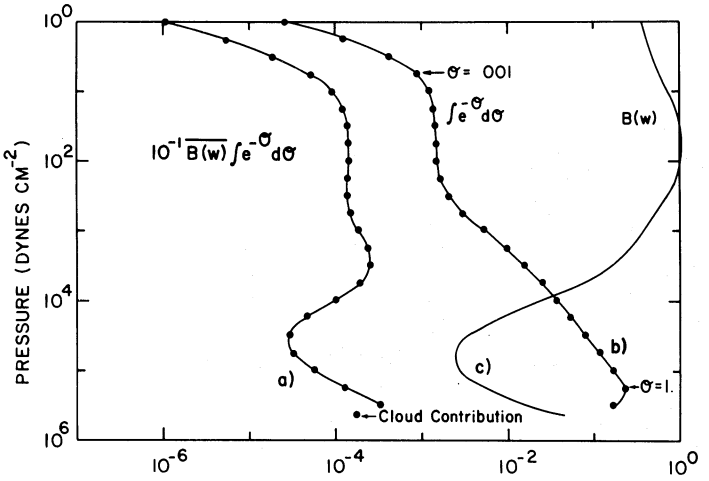

FIG. 9.—Illustration of how the emergent intensity in the 7.8-μ band arises from a wide range of pressures. The curves were calculated from model I (curve *b*, fig. 2) with a cloud at 135° K. They refer to a 20 cm^{-1} band centered at 1240 cm^{-1} (8.056 μ). θ is the slant opacity at an angle of 60°, and $B(\omega)$ is the Planck function. The units on the abscissa for curves (*a*) and (*c*) are ergs $(cm^2\ s\ sr\ cm^{-1})^{-1}$; curve (*b*) is dimensionless on the abscissa.

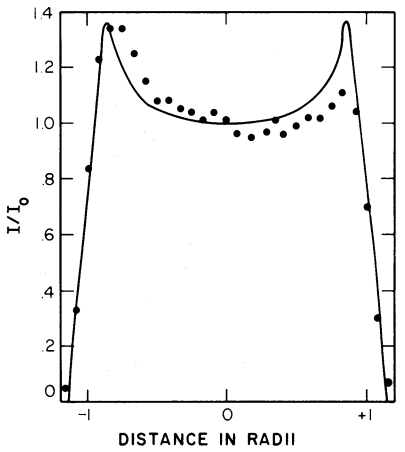

FIG. 10.—Comparison of the center-to-limb observations of Gillett and Westphal (1973) at 7.94 μ with that obtained from model I. The observations and predictions are given by the filled circles and solid line, respectively. In the observations the east limb is at the left.

integrals in which the pressure changes by a factor of $10^{1/4}$. The Planck function in each integral is replaced by its value at the mean pressure:

$$I(\omega, \mu, 0) = \sum_i B[\omega, (p_i p_{i+1})^{1/2}] \int_{P_i}^{P_{i+1}} d\{\exp(-\theta(\omega, \mu, 0, p'))\} . \quad (13)$$

The individual contributions are represented by filled circles connected by a solid curve. While the integral over the opacity (curve *b*) falls off nicely from its peak near $\theta = 1$, the increase in the Planck function (curve *c*) in the region of the temperature inversion is so large as to produce substantial contributions to the intensity (curve *a*) at pressures as low as 10 dyn cm^{-2}. While $\theta = 1$ occurs at a pressure of about 2×10^5 dyn cm^{-2}, half of the emission arises at pressures less than 10^3 dyn cm^{-2}.

Ohring (1973) has inverted the spectrum of Gillett *et al.* for the temperature structure. His results indicate a temperature inversion but at substantially higher pressures than ours, similar to the incorrect results of Hogan *et al.* It is clear, however, from Ohring's discussion that he has neglected the possibility of high-altitude contributions to the methane intensities such as are illustrated in figure 9. He might have achieved this by assuming, for example, that the atmosphere was isothermal above the lowest pressure at which he determined a temperature, as Taylor (1972*b*) did in testing a similar inversion technique. In any case, the result of neglecting a large high-altitude contribution must be to increase the temperatures at lower altitude. Thus Ohring's result represents only one of a family of solutions for the thermal structure and not necessarily the correct one.

The spectrum at wavelengths short of 7 μ is too complex to be considered here. We note only that if the cloud hypothesis has any validity in the 8- to 13-μ region, it must be violated at 5 μ in order to accommodate the high brightness temperatures sometimes observed there (e.g., Keay *et al.* 1973). F. W. Taylor has suggested a model which has a ~90 percent cloud cover and the rest clear. This maintains the constant-brightness-temperature character between 8 to 12 μ, and allows high-temperature radiation to emerge from great depths at 5 μ.

b) Center-to-Limb Variation in the 7.8-μ Methane Band

The variation observed by Gillett and Westphal (1973) at 7.94 μ is compared in figure 10 with the variation predicted by model I. We have assumed a spectral resolution of 20 cm^{-1} and a spatial resolution of 0.35 Jovian radii. The agreement is quite satisfactory. The stated spatial resolution was 0.22 Jovian radii, but our choice of 0.35 gives much better agreement with the observations off the geometric limb. The difference between the two fields of view may possibly be due to seeing and/or an uncertainty in the radial scale.

c) The Effect of Ethane, Ethylene, and Acetylene on the Temperature Structure

In a study of the methane photolysis in the atmosphere of Jupiter, Strobel (1973*a*) concluded that considerable amounts of C_2H_6, C_2H_4, and C_2H_2 would be produced. Recently Ridgway (1974) has obtained high-resolution Jupiter spectra which show in emission the 12.2-μ ethane band and probably the 13.7-μ band of acetylene. While these emissions are weak enough that the low-resolution measurements of Gillett *et al.* (1969) are still representative of the continuum in this region, the real atmosphere is clearly more complicated than the models we have considered here.

TABLE 2

ESTIMATES OF POSSIBLE HIGH-ALTITUDE TEMPERATURES (° K) COMPARED WITH ESTIMATES OF THE TEMPERATURE MINIMA $T^{(0)}$ AND T_e

Planet	$T(CH_4)$	$T(C_2H_6)$	$T(C_2H_4)$	$T^{(0)}$	T_e
Jupiter	154	144	109	109	134*
Saturn	140	125	99	79	97*
Uranus	127	109	90	44	54†
Neptune	120	101	85	35	43†

* Aumann *et al.* 1969.

† $280(1 - A)^{1/4}/R^{1/2}$, with A, the Bond albedo, taken as 0.5.

The effect of these molecules on the thermal structure can be crudely assessed by considering what temperature each of the hydrocarbons would assume at the top of the atmosphere in the optically thin limit. Assuming LTE, the radiative balance is given by

$$\sum S_\omega B_\omega = \frac{1}{4R^2} \sum S_\omega F_\omega \,, \tag{14}$$

from which this temperature can be computed. The summations need only include fundamental bands for which the intensities S_ω have been measured. B_ω and πF_ω are the Planck function and the solar flux at 1 a.u., and R is the planetary distance in a.u. In order to get some idea of the magnitude of the temperature inversion, we note that at some depth a temperature minimum will probably occur which is less than T_e but greater than the minimum temperature $T^{(0)}$ that one would obtain in the absence of the hydrocarbons. In a gray atmosphere the latter temperature is equal to $0.811T_e$, and we take this value as representative of the temperature minimum.

The calculations for methane, ethane, and ethylene are based on band intensities measured by Armstrong and Welsh (1960), Nyquist *et al.* (1957), and Golike *et al.* (1956) and include the 3.3- and 7.8-μ bands of methane, the 3.4-, 6.9-, and 12.2-μ bands of ethane, and the 3.3-, 6.9-, and 10.5-μ bands of ethylene. Acetylene is not included because the required band intensities are not available. The results shown in table 2 indicate that temperature inversions should be the rule, and not the exception, for the outer planets and that the effect of the higher hydrocarbons is to cool the inversion. The results also indicate that the presence of a large amount of ethane could cool the upper Jovian atmosphere by 10° K or so and might degrade the agreement between the predicted and observed intensity of the 7.8-μ band for model I. However, the effect is probably minor since spectral observations, indicate that methane is the predominant hydrocarbon. Nevertheless, models which include ethane and acetylene are clearly of interest.

d) Comparison with Optical Occultation Results

Observations of the occultation of β Sco by Jupiter on 1971 May 13 yield profiles of refractivity which, for an assumed mean molecular mass and an assumed temperature structure of the *overlying* atmosphere, provide temperature as a function of pressure. In figure 11 we compare some of the published occultation results with the models previously shown in figure 5. Small differences in $[He]/[H_2]$ in the various results are not of great consequence.

The models with methane heating alone seem to be most consistent with the occultation results with the exception that they do not show a steep enough temperature gradient between 10 and 10^2 dyn cm^{-2}. In principle, at least, better agreement could be achieved with an additional source of cooling which was important at 10 but not at 10^2 dyn cm^{-2}.

Elliot *et al.* (1974) have recently obtained $[He]/[H_2] = 0.35(+0.37, -0.30)$ from the delay times of the spikes in the occultation curves of β Sco, and a preliminary assessment of the *Pioneer 10* infrared measurements by Chase *et al.* (1974) indicates that $[He]/[H_2]$ may be as high as ~ 0.7. If $[He]/[H_2]$ were as large as 0.5, the occultation temperatures and pressures in figure 11 would have to be increased by factors of ~ 1.3 and ~ 1.8, respectively. The effect on the model profiles is roughly to increase the pressure scale by a factor of 2. Thus increasing the He abundance would require substantially more heating than methane alone can provide in order to maintain agreement with the occultation results. However, we have already seen that higher temperatures would increase the emission intensity in the 7.8-μ region above what is observed. We estimate that if $[He]/[H_2] = 0.5$ and if the temperature increases between 10 and 10^2 dyn cm^{-2} as indicated by the occultation data, the intensity in the 7.8-μ band would be a factor of 30 greater than observed.

The 7.8-μ intensities depend strongly on the peak temperatures but only weakly on the amount of CH_4. To illustrate this, we found it necessary to decrease $[CH_4]/[H_2]$ to 10^{-7} before the factor of 30 discrepancy in the band intensity noted in the previous paragraph was removed. Since the $[CH_4]/[H_2]$ ratios derived from the $3\nu_3$ methane band and the 3–0 and 4–0 quadrupole lines of H_2 (Owen and Mason 1968; Belton 1969; Fink and Belton 1969) are within a factor of 1.5 of the solar abundance ratio of 7×10^{-4}, a mixing ratio of 10^{-7} is quite unreasonable. Thus, for the observed $[CH_4]/[H_2]$ ratio, rough agreement between the models and both the emission intensity in the 7.8-μ region and the β Sco occultation is best obtained for low values ($\ll 0.5$) of $[He]/[H_2]$.

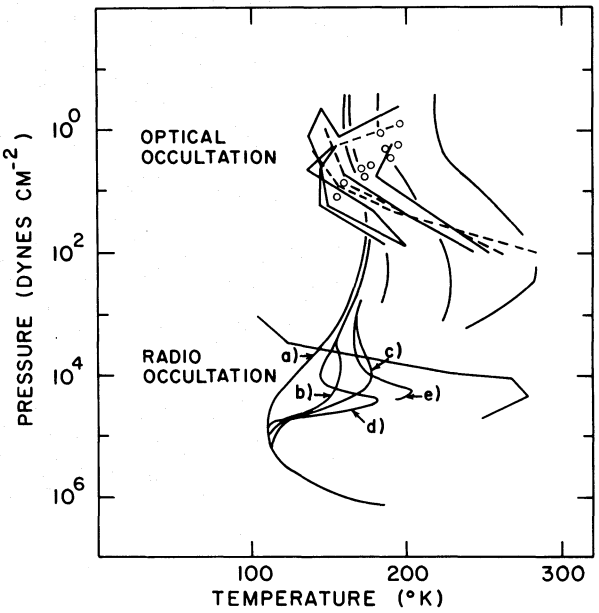

FIG. 11.—Comparison of various models with occultation results. The upper part, above about 10^3 dynes cm^{-2}, shows the results of the optical occultation of β Sco. The broken solid curves represent the models shown in fig. 5. For the optical occultation, the solid-straight line segments are based on the results of Hubbard *et al.* (1972); the dashed straight-line segments represent some of the results of Vapillon *et al.* (1974); and the open circles represent maxima, minima, and inflection points from the results of Veverka *et al.* (1974). The first and third of these are for $[He]/[H_2] = 0.0$; the second, for 0.11. The lower part of the figure shows the results of the *Pioneer 10* radio occultation for an assumed mixing ratio of 0.18. The model curves are those of fig. 7.

e) Comparison with Radio Occultation Results

A preliminary temperature profile has been derived from the closed-loop entry data of the *Pioneer 10* *S*-band occultation experiment by Kliore *et al.* (1974) for $[He]/[H_2] = 0.18$. This profile, converted to a pressure scale, is also shown in figure 11. The models and observations are in clear contradiction. Such a temperature profile does not appear to be achievable with the available solar heating.

More important, perhaps, is the gross conflict between the intensity of the 7.8-μ band which the occultation profile implies and the observed intensity of that band. This can be established by an elementary calculation in which the *Pioneer 10* profile is approximated by an isothermal layer at 260° K between pressures of 10^{-2} and 4×10^{-2} dyn cm^{-2}. The contribution to the intensity from higher and lower pressures is neglected, so a conservative estimate is thus provided. From equation (1), the emergent intensity is

$$I = B(T_1 - T_2)\,, \tag{15}$$

where B is the Planck function at 260° K and 7.8 μ and T_1 and T_2 are the transmissions from the top of the atmosphere down to the pressure of 10^{-2} and 4×10^{-2} dyn cm^{-2}. Transmissions can be obtained from Taylor (1972*a*) and Burch and Williams (1962). With $[CH_4]/[H_2]$ in solar abundance, both predict intensities in the 7.8-μ band of the order of 100 times greater than observed. Such a large discrepancy cannot be removed by reasonable adjustments in either $[CH_4]/[H_2]$ or $[He]/[H_2]$. Consequently, the *Pioneer 10* entry given by Kliore *et al.* (1974), for a solar zenith angle of about 81°, cannot be representative of the global average. If the high-temperature character were restricted to the terminator region or occurred only rarely in the central part of the disk observable from the Earth, it might be possible to remove the conflict.

We are indebted to R. W. Milkey and D. M. Hunten for many helpful discussions of this work.

REFERENCES

Aitken, D. K., and Jones, B. 1972, *Nature*, **240**, 230.
Anderson, R. C., Pipes, J. G., Broadfoot, A. L., and Wallace, L. 1969, *J. Atmos. Sci.*, **26**, 874.
Armstrong, R. L., and Welsh, H. L. 1960, *Spectrochim. Acta*, **16**, 840.
Aumann, H. H., Gillespie, C. M., Jr., and Low, F. J. 1969, *Ap. J. (Letters)*, **157**, L69.
Axel, L. 1972, *Ap. J.*, **173**, 451.
Belton, M. J. S. 1969, *Ap. J.*, **157**, 469.
Belton, M. J. S., and Spinrad, H. 1973, *Ap. J.*, **185**, 363.
Burch, D. E., and Williams, D. 1962, *Appl. Optics*, **1**, 587.
Cess, R. D., and Khetan, S. 1973, *J. Quant. Spectrosc. and Rad. Transf.*, **13**, 995.
Chase, S. C., Ruiz, R. D., Münch, G., Neugebauer, G., Schroeder, M., and Trafton, L. M. 1974, *Science*, **183**, 315.
Danielson, R. E. 1966, *Ap. J.*, **143**, 949.

Elliot, J. L., Wasserman, L. H., Veverka, J., Sagan, C., and Liller, W. 1974, *Ap. J.*, **190**, 719.
Encrenaz, T. 1972, *Astr. and Ap.*, **16**, 237.
Fink, U., and Belton, M. J. S. 1969, *J. Atmos. Sci.*, **26**, 952.
French, R. G., and Gierasch, P. J. 1974, preprint.
Gierasch, P. J. 1970, *Icarus*, **13**, 25.
Gille, J. C., and Lee, T.-H. 1969, *J. Atmos. Sci.*, **26**, 932.
Gillett, F. C., Low, F. J., and Stein, W. A. 1969, *Ap. J.*, **157**, 925.
Gillett, F. C., and Westphal, J. A. 1973, *J. Quant. Spectrosc. and Rad. Transf.*, **13**, 995.
Golike, R. C., Mills, I. M., Person, W. B., and Crawford, B., Jr. 1956, *J. Chem. Phys.*, **25**, 1266.
Goody, R. M. 1964, *Atmospheric Radiation. I. Theoretical Basis* (Oxford: Clarendon Press).
Hogan, J. S., Rasool, S. I., and Encrenaz, T. 1969, *J. Atmos. Sci.*, **26**, 898.
Hubbard, W. B., Nather, R. E., Evans, D. S., Tull, R. G., Wells, D. C., Van Citters, G. W., Warner, B., and Vanden Bout, P. 1972, *A.J.*, **77**, 41.
Hunten, D. M., and Münch, G. 1973, *Space Sci. Rev.*, **14**, 433.
Keay, C. S. L., Low, F. J., Rieke, G. H., and Minton, R. B. 1973, *Ap. J.*, **183**, 1063.
Kliore, A., Cain, D. L., Fjelbo, G., Seidel, B. L., and Rasool, S. I. 1974, *Science*, **183**, 323.
Kuiper, G. P., and Cruikshank, D. P. 1964, *Comm. Lunar and Planet. Lab.*, **2**, 141.
Kyle, T. G. 1968, AFCRL Scientific Report N70-13230.
Labs, D., and Neckel, H. 1968, *Zs. f. Ap.*, **69**, 1.
Linsky, J. L. 1969, *Ap. J.*, **156**, 989.
Nyquist, I. M., Mills, I. M., Person, W. B., and Crawford, B., Jr. 1957, *J. Chem. Phys.*, **26**, 552.
Ohring, G. 1973, *Ap. J.*, **184**, 1027.
Owen, T., and Mason, H. P. 1968, *Ap. J.*, **154**, 317.
Pilcher, C. B., Prinn, R. G., and McCord, T. B. 1973, *J. Atmos. Sci.*, **30**, 302.
Ridgway, S. T. 1974, *Ap. J. (Letters)*, **187**, L41.
Schubert, G., and Young, R. E. 1970, *J. Atmos. Sci.*, **27**, 523.
Stone, P. H. 1972, *J. Atmos. Sci.*, **29**, 405.
Strobel, D. F. 1973*a*, *J. Atmos. Sci.*, **30**, 489.
———. 1973*b*, *ibid.*, **30**, 1205.
Taylor, F. W. 1972*a*, *J. Quant. Spectrosc. and Rad. Transf.*, **12**, 1151.
———. 1972*b*, *J. Atmos. Sci.*, **29**, 950.
Trafton, L. M. 1965, Ph.D. thesis, California Institute of Technology.
———. 1966, *Ap. J.*, **146**, 558.
———. 1967, *ibid.*, **147**, 765.
———. 1973, *J. Quant. Spectrosc. and Rad. Transf.*, **13**, 821.
Trafton, L. M., and Stone, P. H. 1974, *Ap. J.*, **188**, 649.
Vapillon, L., Combes, M., and Lecacheux, J. 1974, *Astr. and Ap.*, in press.
Varanasi, P. 1971, *J. Quant. Spectrosc. and Rad. Transf.*, **11**, 1711.
———. 1972, *ibid.*, **12**, 1283.
Varanasi, P., and Tejwani, G. D. T. 1972, *J. Quant. Spectrosc. and Rad. Transf.*, **12**, 849.
Veverka, J., Wasserman, L. H., Elliot, J., Sagan, C., and Liller, W. 1974, preprint.
Wallace, L., Caldwell, J. J., and Savage, B. D. 1972, *Ap. J.*, **172**, 755.
Wallace, L., and Hunten, D. M. 1973, *Ap. J.*, **182**, 1013.
Wasserman, L., and Veverka, J. 1973, *Icarus*, **20**, 322.

MICHAEL J. S. BELTON and L. WALLACE: Kitt Peak National Observatory, P.O. Box 26732, Tucson, AZ 85726
MICHAEL PRATHER: Yale University, Astronomy Dept., Box 2023, Yale Station, New Haven, CT 06520